

**Global distribution of
CCN uncertainty**

L. A. Lee et al.

Title Page

Abstract

Introduction

Conclusions

References

Tables

Figures

◀

▶

◀

▶

Back

Close

Full Screen / Esc

Printer-friendly Version

Interactive Discussion



This discussion paper is/has been under review for the journal Atmospheric Chemistry and Physics (ACP). Please refer to the corresponding final paper in ACP if available.

Mapping the uncertainty in global CCN using emulation

L. A. Lee, K. S. Carslaw, K. J. Pringle, and G. W. Mann

Institute for Climate and Atmospheric Science, School of Earth and Environment, University of Leeds, UK

Received: 11 April 2012 – Accepted: 25 May 2012 – Published: 6 June 2012

Correspondence to: L. A. Lee (l.a.lee@leeds.ac.uk)

Published by Copernicus Publications on behalf of the European Geosciences Union.

Abstract

In the last two IPCC assessment reports aerosol radiative forcings have been given the largest uncertainty range of all forcing agents assessed. This forcing range is really a diversity of simulated forcings in different models and an essential step towards reducing it is to quantify and attribute sources of model uncertainty at the process level. Here, we use statistical emulation techniques to quantify uncertainty in simulated concentrations of July-mean cloud condensation nuclei (CCN) from a complex global aerosol microphysics model. Specifically, we use Gaussian process emulation to give a full variance-based sensitivity analysis and quantify, for each model grid box, the uncertainty in simulated CCN that results from 8 uncertain model parameters. We produce global maps of absolute and relative CCN sensitivities to the 8 model parameter ranges and derive probability density functions for simulated CCN. The approach also allows us to include the uncertainty from interactions between these parameters, which cannot be quantified in traditional one-at-a-time sensitivity tests. The key findings from our analysis are that model CCN in polluted regions and the Southern Ocean are mostly only sensitive to uncertainties in emissions parameters but in all other regions CCN uncertainty is driven almost exclusively by uncertainties in parameters for model processes. For example, in marine regions between 30° S and 30° N model CCN uncertainty is driven mainly by parameters associated with cloud-processing of Aitken-sized particles whereas in polar regions uncertainties in scavenging parameters dominate. In these two regions a single parameter dominates but in other regions up to 50 % of the variance can be due to interaction effects between different parameters. Our analysis provides direct quantification of the reduction in variance that would result if a parameter could be specified precisely. When extended to all process parameters the approach presented here will therefore provide a clear global picture of how improved knowledge of aerosol processes would translate into reduced model uncertainty.

Global distribution of CCN uncertainty

L. A. Lee et al.

Title Page

Abstract

Introduction

Conclusions

References

Tables

Figures

◀

▶

◀

▶

Back

Close

Full Screen / Esc

Printer-friendly Version

Interactive Discussion



1 Introduction

Many of the atmospheric processes that control and shape the global aerosol distribution cannot be explicitly treated in models, either due to a lack of understanding or through computational constraints. Treatment of these processes in models thus relies on simplified parameterisations, which often contain parameters that are not well constrained by measurements or theory. This parametric uncertainty means that every model simulation has some degree of uncertainty associated with it. Although one-at-a-time sensitivity tests are commonly used to estimate the range of model predictions, these are far from adequate for estimating the associated confidence interval around the model since no parameter interactions can be taken into account. Rather, most effort to define uncertainty has focused on multi-model inter-comparisons (Schimel et al., 1996; Penner et al., 2001; Forster et al., 2007; Textor et al., 2006, 2007; Meehl et al., 2007), which provide an important insight into model diversity, but no estimate of the parametric uncertainty of the individual models. In our study, we focus on parameter uncertainty in a single model, quantifying and attributing uncertainties in simulated CCN concentrations from several uncertain model parameters.

Sensitivity analysis (SA) offers a way of quantifying model uncertainty and identifying which processes contribute most to it. SA is usually carried out using standard “one-at-a-time” (OAT) sensitivity tests which systematically investigate departures of model behaviour from some baseline. However, OAT tests cannot identify and quantify non-linear behaviour and they consider only a small fraction of the total parameter uncertainty space (Saltelli and Annonia, 2010). A more comprehensive approach is to use Monte Carlo simulations in which the statistical distribution of the model output is populated by sampling thousands of possible parameter values across the multi-dimensional parameter uncertainty space. The output distribution is then used for the sensitivity analysis, such as analysis of variance and variance decomposition to understand contributions to the overall variance. However, Monte Carlo simulation requires

Global distribution of CCN uncertainty

L. A. Lee et al.

Title Page

Abstract

Introduction

Conclusions

References

Tables

Figures

◀

▶

◀

▶

Back

Close

Full Screen / Esc

Printer-friendly Version

Interactive Discussion



a very large number of model simulations, which is normally prohibitively expensive for complex atmospheric models.

We use emulation to carry out a parametric sensitivity analysis of a global aerosol model. An emulator is a statistical interpolator which takes the output of model simulations spread throughout the parameter uncertainty space and estimates the output throughout the rest of the space using conditional probability theory. We describe the methodology of emulation in detail in Lee et al. (2011) (hereafter Lee11) where we presented the first application of Gaussian process emulation for sensitivity analysis of a global aerosol model. The results presented in this work use the same GLOMAP simulations as presented in Lee11 and vary the same 8 uncertain parameters (detailed below), but in this work we use different computational software to enable analysis of every model gridbox to provide global maps (Lee11 was restricted to analysis of two gridboxes). As with Lee11 we emulate the simulated cloud condensation nuclei concentration, the subset of the aerosol population that can form cloud droplets. This is a key quantity in the prediction of the aerosol indirect effect. The advantage of extending the analysis from point locations to the global scale is clear: it allows the identification of regions where parametric uncertainty strongly affects CCN and identifies the role of the different parameters in different regions.

2 Aerosol model description

The GLObal Model of Aerosol Processes (GLOMAP-mode) (Mann et al., 2010) simulates the size distribution and composition of a population of aerosol particles. The model includes new particle formation, coagulation, gas-to-particle transfer and cloud processing. GLOMAP-mode treats the aerosol size distribution using 7 lognormal modes (soluble nucleation, Aitken, accumulation and coarse modes plus water-insoluble Aitken, accumulation and coarse modes for initially insoluble soot and dust particles). GLOMAP-mode is implemented within the TOMCAT global 3-D offline chemistry transport model (Chipperfield, 2006). The model is run with the same setup as

Global distribution of CCN uncertainty

L. A. Lee et al.

Title Page

Abstract

Introduction

Conclusions

References

Tables

Figures

◀

▶

◀

▶

Back

Close

Full Screen / Esc

Printer-friendly Version

Interactive Discussion



described in detail by (Mann et al., 2010). It includes sea spray, black carbon, organic carbon and dust and has been shown to compare well with ground based observations of aerosol mass and number (Mann et al., 2010; Spracklen et al., 2010). The model resolution is $2.81 \times 2.81^\circ$ with 31 vertical levels.

5 The model was spun up for three months before any parameter perturbation was applied. After perturbation, a further 2 months of spin up was permitted and the analysis was done on the third month after perturbation, in this case July 2000. At the resolution used here GLOMAP-mode takes about 1.4 h to run per month on 32 cores.

3 Statistical methods

10 The experimental design and emulator validation are outlined in detail in Lee11, but for clarity we recap some of the methodology here.

The emulator used here is a non-parametric emulator based on the well-established statistical theory of the Gaussian process (O'Hagan, 2006). Gaussian process emulation is a Bayesian technique in which the prior probability distribution of the GLOMAP output is conditioned on some model-simulated output to produce a posterior probability distribution for the output. With the (unknown) July CCN defined by Y , the uncertain parameters defined by $X = \{X_1, \dots, X_8\}$ and GLOMAP defined as the function η we have $Y = \eta(X)$. The model simulated output (training data) is $y_1 = \eta(x_1), \dots, y_{80} = \eta(x_{80})$. We use emulation to estimate η by $\hat{\eta}$ and use this to perform the sensitivity analysis. The prior distribution is the Gaussian process with mean $m(x) = h(x)^T \beta$ where $h(\cdot)$ is a known function of x with unknown coefficients β . In this work $h(\cdot)$ is the simple linear regression function and the coefficients calculated using the training data. The prior covariance function is $\text{cov}(x, x') = \sigma^2 c(x, x')$ where $c(x, x') = \exp\{-\sum_{i=1}^8 \left(\frac{(x_i - x'_i)}{\delta_i}\right)^2\}$ is the Gaussian correlation function depending on the distance between pairs of points and the smoothness of the model response to each parameter defined by δ calculated from the training data. The resulting emulator is a conditional probability distribution

Title Page

Abstract

Introduction

Conclusions

References

Tables

Figures

◀

▶

◀

▶

Back

Close

Full Screen / Esc

Printer-friendly Version

Interactive Discussion



Global distribution of CCN uncertainty

L. A. Lee et al.

Title Page

Abstract

Introduction

Conclusions

References

Tables

Figures

◀

▶

◀

▶

Back

Close

Full Screen / Esc

Printer-friendly Version

Interactive Discussion



for η representing the behaviour of a given GLOMAP output given the chosen inputs with mean $m^*(x) = h(x)^T \hat{\beta} + t(x)^T A^{-1}(y - H\hat{\beta})$ and covariance matrix $\text{cov}^*(x, x') = \sigma^2 [c(x, x') - t(x)^T A^{-1} t(x') + (h(x) - t(x)^T A^{-1} H)(H^T A^{-1} H)^{-1} (h(x') - t(x')^T A^{-1} H)^T]$. The details of these equations can be found in Lee11. The emulator provides an estimate of the model output at any point x in the parameter uncertainty space with uncertainty. The more information from model simulations that is used to produce the emulator the smaller the emulator uncertainty will be, so the reduction in uncertainty due to emulation has to be balanced with the increased efficiency from using emulation rather than direct simulation. The emulator is validated by comparing emulator predictions and its uncertainty, $m^*(x) \pm 2 \times \sqrt{\text{cov}^*(x, x)}$, to actual GLOMAP output, $\eta(x)$, at some previously untried parameter settings x (see Lee11). If the emulator is deemed valid according to some defined critical level then the areas of parameter space that were not covered by the GLOMAP simulations can be investigated using the emulator with no need for further model simulations. The sensitivity analysis is therefore carried out using the emulator mean $m^*(x)$ conditioned on GLOMAP.

The sensitivity analysis used here is the extended-FAST (Fourier Amplitude Sensitivity Test) method (Saltelli et al., 1999) which calculates two measures of sensitivity based on the variance of $m^*(x)$ after sampling x from the 8-dimensional uncertainty space:

The main effect measures the reduction in the output variance if the parameter could be learnt exactly. This is the output sensitivity to each parameter alone.

The total effect measures the reduction in the output variance when everything but the parameter is learnt. This is the output sensitivity to each parameter and its interactions.

The emulator is built using the statistical software R (R Development Core Team, 2011) with the package DiceKriging (Roustant et al., 2011) and sensitivity analysis is carried out using the package sensitivity (Pujol, 2008).

The sensitivity analysis here focuses on the scalar monthly mean cloud condensation nuclei (CCN) concentration on the 915 hPa altitude level of the model and quantifies its sensitivity to 8 model parameters. This model level was chosen because this is around the altitude of cloud base and therefore the impact of changes in CCN will be relevant for the radiative properties of clouds and the indirect forcing. The 8 model parameters were identified in a previous model sensitivity study Spracklen et al. (2005) as potentially important. We recognise that 8 parameters is only a subset of the total parameter uncertainty but here we demonstrate the technique of emulation of CCN on a global scale for the first time. As in Lee11 no formal elicitation was done. The parameters and their uncertainty limits are summarised in Table 1. Eighty model runs were used to train the emulator, with points in 8-dimensional parameter space defined by a Latin-Hypercube maximin algorithm (McKay et al., 1979). The simulations took 351 h on 32 cores, or nearly 15×32 core-days. The same 80 models runs were used in Lee11.

4 Results

4.1 CCN parametric uncertainty

Figure 1 shows the emulated mean CCN and standard deviation in every surface grid box resulting from uncertainty in the 8 model parameters as described above. Also shown for comparison is the mean CCN from the 80 GLOMAP simulations in the experimental design. Results are shown for July 2000. Figure 1 shows that emulated mean CCN concentrations are very close to the mean simulated CCN, as expected given the uniform input parameter uncertainty distributions used here and a sufficient experimental design. Figure 1c shows posterior CCN distributions for 13 locations, illustrating that the emulator does not necessarily produce symmetric CCN distributions, even though the input parameter uncertainties were uniform. A range of distributional shapes can be seen, with remote regions having strongly skewed pdf, with a long tail

Global distribution of CCN uncertainty

L. A. Lee et al.

Title Page

Abstract

Introduction

Conclusions

References

Tables

Figures

◀

▶

◀

▶

Back

Close

Full Screen / Esc

Printer-friendly Version

Interactive Discussion



of low probability high CCN concentrations. These posterior CCN distributions were produced by sampling 80 000 points from the emulator mean function and not from the 80 model simulations. Although 80 simulations sounds a lot, it is actually far less than is required to generate statistically reliable probability distributions or to perform a full variance-based sensitivity analysis as we do in the next section. The number of runs typically required to produce statistically reliable results is discussed in O'Hagan (2006) and the number of runs required to produce the sensitivity measures with the extended-FAST method is discussed in Cukier et al. (1977).

The highest CCN concentrations over polluted areas correlate with the regions of highest absolute uncertainty. In contrast, the coefficient of variation (Fig. 2) shows the opposite pattern, with the highest values over remote regions. The coefficient of variation reaches a maximum at high latitudes where the uncertainty is 50–80 % of the CCN concentration. The apparent very low CCN uncertainty over South Africa and South America is likely only due to those regions being dominated by biomass burning emissions parameters, which were not included in the 8 chosen parameters here. A future study will cover a much more complete set of uncertain model parameters, with expert elicitation used to ensure all important processes are considered.

4.2 CCN sensitivity to individual parameters

In order to identify how the CCN can be better constrained, we carry out sensitivity analysis to quantify the relative contribution of each of the parameter uncertainties to the overall CCN uncertainty in Fig. 1. The main effect contributions of each parameter to the CCN variance are shown in Fig. 3 and the corresponding absolute standard deviation in Fig. 4. Figure 3 shows the relative importance of uncertainty in different processes in different global regions. Note that the effect of a given parameter on the CCN uncertainty in any grid box does not imply that the process is localised to that grid box. The aerosol in any location has undergone long-range transport and transformation, so the parameter sensitivity in a given grid box depends on the integrated effect of the uncertain parameter over the lifecycle of the aerosol during transport.

Global distribution of CCN uncertainty

L. A. Lee et al.

Title Page

Abstract

Introduction

Conclusions

References

Tables

Figures

◀

▶

◀

▶

Back

Close

Full Screen / Esc

Printer-friendly Version

Interactive Discussion



**Global distribution of
CCN uncertainty**

L. A. Lee et al.

[Title Page](#)[Abstract](#)[Introduction](#)[Conclusions](#)[References](#)[Tables](#)[Figures](#)[◀](#)[▶](#)[◀](#)[▶](#)[Back](#)[Close](#)[Full Screen / Esc](#)[Printer-friendly Version](#)[Interactive Discussion](#)

The main contributors to CCN uncertainty in the Southern Ocean and polar regions are uncertainty in the scavenging diameter (the size above which particles are assumed to be nucleation scavenged in precipitating gridboxes) and the sea spray emissions, which account for over 60 % of the variance throughout these regions. These are also the regions with the greatest coefficient of variation (Fig. 2). The areas of highest uncertainty in CCN in Fig. 1 are dominated by the $\pm 30\%$ uncertainty in the SO_2 emissions, which accounts for over 70 % of the variance in regions dominated by anthropogenic sulphur emissions. Two of the chosen parameters, the nucleation critical cluster size and the fraction of anthropogenic SO_2 emissions to be emitted in particulate form, lead to $< 10\%$ of the variance in CCN concentrations and are hence considered insensitive, Fig. 4 shows that the absolute standard deviation in CCN from uncertainty in these two parameters is also small. The lack of sensitivity to sub-grid particulate SO_4 emissions is surprising as previous work has shown sensitivity to this parameter (Adams and Seinfeld, 2003). However, in these simulations we followed Stier et al. (2005) and emitted at a larger size than Adams and Seinfeld (2003), thus the sensitivity is much less. In the next experiment, the size, as well as the emission rate, of the particulates will be investigated based on new information from detailed plume studies (Stevens et al., 2012).

The mid tropical oceans are dominated by uncertainty in the oxidation activation diameter (the size above which soluble particles are assumed to activate to cloud droplets in stratiform cloud), which accounts for nearly 90 % of the variance in this region. The absolute standard deviation contribution map (Fig. 4) shows that this process is most important over the regions of persistent marine stratocumulus clouds (e.g., off the west coast of Namibia and Central America).

Whereas in polluted regions, the CCN uncertainty is mainly from SO_2 emissions, in less-polluted continental regions, CCN are more sensitive to the uncertainties in the accommodation coefficient and nucleation threshold, which have a similar spatial pattern. The nucleation threshold controls nucleation in the free troposphere (FT) due to binary homogeneous nucleation (Kulmala et al., 1998; Spracklen, 2005). Merikanto et al.

(2009) showed that FT nucleation is a significant source of CCN to the boundary layer (the altitude that we analyse here). The impact of this nucleation on boundary layer CCN depends on the growth of the nuclei to CCN sizes during downward transport and mixing, which is mainly driven by sulphuric acid condensation, hence the mass accommodation coefficient (ACC_COEF in Fig. 3). The result is consistent with Merikanto et al. (2009) where it was shown that the FT CCN source is amplified over land areas because the particles grow more rapidly due to uptake of the available biogenic SOA and anthropogenic sulphuric acid over polluted continental regions.

It is important to distinguish between the importance of a parameter in controlling the mean CCN concentration and its importance in controlling the uncertainty in CCN. A process or emission has to make a significant contribution to CCN for the CCN to be sensitive to parameters controlling that process, but the converse is not necessarily true; i.e., an emission could be a major source of CCN but the CCN concentration could be relatively insensitive to variations in those emissions. The nucleation threshold seems to be a parameter that behaves like this. In Merikanto et al. (2009) we showed that FT nucleation is a major source of boundary layer CCN, accounting for up to 80% of CCN over marine regions between 30° S and 30° N. However, in Fig. 3, NUC_THRESH contributes to CCN variance mainly over land areas. A plausible explanation is that over marine regions there is very little condensable vapour to grow the nuclei to CCN sizes, so growth is mainly through coagulation, which reduces particle concentrations and suppresses the sensitivity to the initial nucleation rate. Thus, FT nucleation makes a large contribution to mean boundary layer CCN concentrations over marine regions, but the concentration is not very sensitive to the nucleation rate in the free and upper troposphere.

4.3 Parameter interactions

By using the emulation approach we are able to investigate the entire parameter uncertainty space and therefore quantify the interactions between the 8 uncertain parameters shown. Interactions indicate non-linear coupling of parameter effects in the

Global distribution of CCN uncertainty

L. A. Lee et al.

Title Page

Abstract

Introduction

Conclusions

References

Tables

Figures

◀

▶

◀

▶

Back

Close

Full Screen / Esc

Printer-friendly Version

Interactive Discussion



5 GLOMAP output. For example, if the total effect variance is equal to the main effect for a given parameter, then that parameter impacts CCN independently of the other parameters and a one-at-a-time test will be sufficient to determine the total sensitivity. Interactions occur when, for example, a high setting of one parameter amplifies or suppresses the sensitivity to another parameter compared to its one-at-a-time sensitivity. Note, however, that the model response to one parameter can still be non-linear over its range even without interactions, but this single-parameter non-linearity is captured in our analysis as part of the main effect variance.

10 Figure 5 shows the percentage of the variance that is not caused by main effect of the parameters and is therefore caused by the interactions between the parameters; this is the percentage of the variance that cannot be quantified using OAT tests. Interactions are important in large regions of the globe including marine tropical regions (particularly in the Northern Hemisphere), Alaska, Siberia, Antarctica, Southernmost South America and South Australia. Interaction effects are negligible (and therefore OAT tests sufficient) over some of the more polluted regions such as Europe and East China. The peak contribution of interaction effects to the total variance is about 50 %, thus OAT tests would underestimate the uncertainty in CCN in these regions by this amount.

20 The contributions of each parameter to the interaction effect are shown in Fig. 6. These were calculated by subtracting the main effect from the total effect for each parameter. By examining the spatial patterns of the interactions it is possible to determine which parameters interact with each other. The largest interaction is between the scavenging diameter and the oxidation activation diameter, which interact with each other or other model parameters throughout most of the globe and account for up to 30 % of the variance. These two parameters clearly account for CCN variance over Northern Hemisphere oceans, in the Arctic and over Alaska. Physically, this interaction can be explained by the effect of cloud processing on the aerosol size distribution, which impacts the scavenging in precipitating clouds. A low setting of the activation diameter in non-precipitating low clouds (the OX_DIAM parameter) leads to cloud processing and

**Global distribution of
CCN uncertainty**

L. A. Lee et al.

Title Page

Abstract

Introduction

Conclusions

References

Tables

Figures

◀

▶

◀

▶

Back

Close

Full Screen / Esc

Printer-friendly Version

Interactive Discussion



growth of a larger fraction of the aerosols, shifting the size distribution to sizes where scavenging can occur in precipitating clouds.

Another strong interaction occurs between sea spray emissions and the scavenging diameter, which is apparent over Southern Australia, Southernmost South America and Antarctica. This large interaction is due to the diminishing sensitivity of the scavenging diameter as the sea spray emissions increase. The other dominant interaction is between the accommodation coefficient of sulphuric acid (ACC_COEF) and the binary homogeneous nucleation threshold (NUC_THRESH). This interaction accounts for up to 30 % of the variance over the Northern Hemisphere land areas. Sulphur emissions do not interact with the other processes considered in this study thus could be investigated using OAT tests.

4.4 Identification of dominant parameters

An understanding of the important processes that control the uncertainty in CCN can help to direct research efforts to the processes of most global importance. Learning the global importance of each parameter and the CCN uncertainty that it contributes means that the value of future research can be quantified.

Figure 7 shows maps of the dominant parameter (of the 8) leading to uncertainty in the CCN concentration and the fraction of CCN variance explained by its total effect (the effect of the parameter individually and all its interactions). The uncertainty in oxidation diameter dominates 35 % of the uncertainty in the boundary layer, scavenging diameter dominates uncertainty in 28 % and sea spray dominates uncertainty in 17 % of the boundary layer. Five of the parameters contribute less than 10 % of the uncertainty through the boundary layer. There is large variation in the fraction of variance explained by the dominant parameter. The simplest regions are dominated by one parameter (scavenging diameter) that controls 70–90 % of the variance in the remote marine regions and > 90 % of the variance in Antarctica. Thus, the CCN variance in July would be reduced by 70–90 % if this parameter could be learnt precisely. There are other regions where only 20–40 % of the variance is explained by the dominant

Global distribution of CCN uncertainty

L. A. Lee et al.

Title Page

Abstract

Introduction

Conclusions

References

Tables

Figures

◀

▶

◀

▶

Back

Close

Full Screen / Esc

Printer-friendly Version

Interactive Discussion



parameter. Over most land areas the dominant parameter accounts for 40% of the CCN variance suggesting the variance is shared between multiple parameters, as can be seen in Fig. 3. The mid-tropical oceans are dominated by uncertainty in the oxidation activation diameter which accounts for between 40 and 100% of the variance but the CCN concentration in this region is reasonably well constrained, with a coefficient of variation of only 0.2–0.3 (Fig. 2).

5 Conclusions

Emulation is a powerful method for understanding the sources of uncertainty in a complex global model. It is based on well established statistical theory with clear and testable assumptions. A relatively small number of model simulations covering the uncertainty space of the parameters generates sufficient information to enable a full variance-based sensitivity analysis to be performed, which would otherwise require an unfeasibly large number of model simulations using a Monte Carlo approach. The emulator is computationally efficient and can therefore be built for every grid box of a global model. Here we have focused on CCN, but similar information could be generated for optical depth or any other quantity based on the existing model runs. The emulator also generates a full probability density function (pdf) of any model output in every grid box, which is not constrained to be Gaussian. Compared to one-at-a-time sensitivity tests the emulator generates vastly more information to aid model development and uncertainty reduction.

Our results show that variance-based analysis of the emulated global model produces spatial patterns of parameter dependencies and interactions that make sense in terms of the processes that control the properties of the aerosol in different regions. There is a high degree of coherence in the patterns, suggesting that the variance analysis is generating physically meaningful information about the response of the model to its uncertain parameters. The spatial distribution of the variance contribution of some parameters is clearly localised to the place where that parameter is acting.

Global distribution of CCN uncertainty

L. A. Lee et al.

Title Page

Abstract

Introduction

Conclusions

References

Tables

Figures

◀

▶

◀

▶

Back

Close

Full Screen / Esc

Printer-friendly Version

Interactive Discussion



For example, the uncertainty in sea spray emissions shows up primarily in windy marine regions. However, the uncertainty in some parameters has a non-local impact on CCN variance. For example, aerosol wet scavenging strongly affects the overall CCN uncertainty in remote non-cloudy regions and the interaction of uncertain sea spray emissions with other parameters influences CCN over Antarctica.

Our approach, which could readily be extended to a larger set of parameters and eventually more models, provides a framework for the quantifiable reduction in model uncertainty and improvement in robustness. A robust model is one that is still reliable when its uncertain parameters are varied. However, robustness cannot be assessed from a very limited set of one-at-a-time parameter perturbations. Model evaluation based on comparing the full pdf of model results against observations will enable model robustness to be tested for the first time.

A complete understanding of the model behaviour within the parameter uncertainties will also aid the next step of reducing model uncertainty: calibration. Calibration, which is widely used in other fields of environmental modelling, is the identification of the model that best matches observations within defined criteria (e.g., of bias, correlation, etc) (Kennedy and O'Hagan, 2001). Aerosol model calibration would be a significant step compared to previous studies that have attempted to identify the best model based on a very small number of model sensitivity tests. In such cases we have no idea whether poor model performance is simply due to neglect of a plausible part of the parameter space, which can now be fully quantified using the emulator.

Our approach could also provide a way to more reliably identify model structural weaknesses and thereby prioritise future model development. Structural weaknesses will become apparent by identifying regions (e.g., free troposphere, Arctic) or conditions (clean, polluted, cloudy) where the model-observation bias is outside the full range of parameter uncertainties (defined by the pdf). Such discrepancies will either indicate that we have not considered all the important parameters (or underestimated their uncertainty range) of the present model or that the model has structural deficiencies such

Global distribution of CCN uncertainty

L. A. Lee et al.

Title Page

Abstract

Introduction

Conclusions

References

Tables

Figures

◀

▶

◀

▶

Back

Close

Full Screen / Esc

Printer-friendly Version

Interactive Discussion



as neglected emissions, incomplete processes or deficiencies in the host transport model.

Global analyses of uncertainty sources could also be used to develop new measurement strategies to maximise the reduction in uncertainty in aerosol forcing. Variance maps can be used to define the location and type of measurements that will have the greatest impact on reducing uncertainty in CCN or any other aerosol quantity. At present, many field campaigns make novel measurements of unexplored aerosol properties and processes but are less steered by the requirement to develop more robust models.

A further extension of the model emulation approach will be to study the importance of interactions, for example in the air quality-climate system. Most mitigation studies focus on the response of atmospheric composition or climate to one parameter at a time (e.g., SO₂ or NO_x emission reductions), although future air quality and climate will be driven by simultaneous changes in many parameters. The emulator results that we have analysed here to quantify variance can also be used to understand the model response surface. This will enable the response of, say, particulate matter, to all possible combinations of emissions changes to be investigated based on a relatively small number of model simulations.

Acknowledgements. We acknowledge funding from the Natural Environment Research Council AEROS project under grant NE/G006172/1 and the EU FP7 IP PEGASOS (FP7-ENV-2010/265148).

References

- Adams, P. J. and Seinfeld, J. H.: Disproportionate impact of particulate emissions on global cloud condensation nuclei concentrations, *Geophys. Res. Lett.*, 30, 1239, doi:10.1029/2002GL016303, 2003. 14097
- Chipperfield, M.: New version of the TOMCAT/SLIMCAT off-line chemical transport model: inter-comparison of stratospheric tracer experiments, *Q. J. Roy. Meteorol. Soc.*, 132, 1179–1203, doi:10.1256/qj.05.51, 2006. 14092

Global distribution of CCN uncertainty

L. A. Lee et al.

Title Page

Abstract

Introduction

Conclusions

References

Tables

Figures

◀

▶

◀

▶

Back

Close

Full Screen / Esc

Printer-friendly Version

Interactive Discussion



- Cukier, R. I., Levine, H. B., and Shuler, K. E.: Nonlinear sensitivity analysis of multiparameter model systems, *J. Phys. Chem.*, 81, 2365–2366, www.scopus.com, cited by (since 1996): 7, 1977. 14096
- Forster, P., Ramaswamy, V., Artaxo, P., Bernsten, T., Betts, R., Fahey, D., Haywood, J., Lean, J., Lowe, D., Myhre, G., Nganga, J., Prinn, R., Raga, G., Schulz, M., and Van Dorland, R.: Changes in atmospheric constituents and in radiative forcing, in: *Climate Change 2007: The Physical Science Basis. Contribution of Working Group I to the Fourth Assessment Report of the Intergovernmental Panel on Climate Change*, edited by: Solomon, S., Qin, D., Manning, M., Chen, Z., Marquis, M., Averyt, K. B., Tignor, M., and Miller, H. L., Cambridge University Press, Cambridge, UK and New York, NY, USA, 2007. 14091
- Kennedy, M. and O'Hagan, A.: Bayesian calibration of computer models (with discussion), *J. Roy. Stat. Soc. B Met.*, 63, 425–464, 2001. 14102
- Kulmala, M., Laaksonen, A., and Pirjola, L.: Parameterizations for sulfuric acid/water nucleation rates, *J. Geophys. Res.*, 103 (D7), 8301–8307, 1998. 14097
- Lee, L. A., Carslaw, K. S., Pringle, K. J., Mann, G. W., and Spracklen, D. V.: Emulation of a complex global aerosol model to quantify sensitivity to uncertain parameters, *Atmos. Chem. Phys.*, 11, 12253–12273, doi:10.5194/acp-11-12253-2011, 2011. 14092
- Mann, G. W., Carslaw, K. S., Spracklen, D. V., Ridley, D. A., Manktelow, P. T., Chipperfield, M. P., Pickering, S. J., and Johnson, C. E.: Description and evaluation of GLOMAP-mode: a modal global aerosol microphysics model for the UKCA composition-climate model, *Geosci. Model Dev.*, 3, 519–551, doi:10.5194/gmd-3-519-2010, 2010. 14092, 14093
- McKay, M., Conover, W., and Beckman, R.: A comparison of three methods for selecting values of input variables in the analysis of output from a computer code, *Technometrics*, 21, 239–245, 1979. 14095
- Meehl, G. A., Covey, C., Delworth, T., Latif, M., McAvaney, B., Mitchell, J., Stouffer, R., and Taylor, K.: The WCRP CMIP3 multi-model dataset: a new era in climate change research, *B. Am. Meteorol. Soc.*, 88, 1383–1394, 2007. 14091
- Merikanto, J., Spracklen, D. V., Mann, G. W., Pickering, S. J., and Carslaw, K. S.: Impact of nucleation on global CCN, *Atmos. Chem. Phys.*, 9, 8601–8616, doi:10.5194/acp-9-8601-2009, 2009. 14097, 14098
- O'Hagan, A.: Bayesian analysis of computer code outputs: a tutorial, *Reliab. Eng. Syst. Safe.*, 91, 1290–1300, 2006. 14093, 14096

**Global distribution of
CCN uncertainty**

L. A. Lee et al.

Title Page

Abstract

Introduction

Conclusions

References

Tables

Figures

◀

▶

◀

▶

Back

Close

Full Screen / Esc

Printer-friendly Version

Interactive Discussion



Global distribution of CCN uncertainty

L. A. Lee et al.

Title Page

Abstract

Introduction

Conclusions

References

Tables

Figures

◀

▶

◀

▶

Back

Close

Full Screen / Esc

Printer-friendly Version

Interactive Discussion



- Penner, J., Andreae, M., Annegarn, H., Barrie, L., Feichter, J., Hegg, D., Jayaraman, A.,
Leaitch, R., Murphy, D., Nganga, J., and Pitar, G.: Aerosols, their direct and indirect effects,
in: *Climate Change 2001: The Scientific Basis. Contribution of Working Group I to the Third
Assessment Report of the Intergovernmental Panel on Climate Change*, edited by:
5 Houghton, J. T., Ding, Y., Griggs, D. J., Noguer, M., van der Linden, P. J., Dai, X., Maskell, K.,
and Johnson, C. A., Cambridge University Press, Cambridge, UK and New York, NY, USA,
2001. 14091
- Pujol, G.: Sensitivity: sensitivity analysis, r package version 1.4-0, last access: 15 December
2011, 2008. 14094
- 10 Roustant, O., Ginsbourger, D., and Deville, Y.: DiceKriging: kriging methods for computer ex-
periments, available at: <http://CRAN.R-project.org/package=DiceKriging>, r package version
1.3.2, last access: 15 December 2011, 2011. 14094
- Saltelli, A. and Annonia, P.: How to avoid a perfunctory sensitivity analysis, *Environ. Modell.
Softw.*, 25 (12), 1508–1517, 2010. 14091
- 15 Saltelli, A., Tarantola, S., and Chan, K. P.-S.: A quantitative model-independent method for
global sensitivity analysis of model output, *Technometrics*, 41, 39–56, doi:10.2307/1270993,
1999. 14094
- Schimel, D., Alves, D., Enting, I., Heimann, M., Joos, F., Raynaud, D., Wigley, T., Prather, M.,
Derwent, R., Ehhalt, D., Fraser, P., Sanhueza, E., Zhou, X., Jonas, P., Charlson, R.,
20 Rodhe, H., Sadasivan, S., Shine, K., Fouquart, Y., Ramaswamy, V., Solomon, S., Sriniva-
san, J., Albritton, D., Derwent, R., Isaksen, I., Lal, M., and Wuebbles, D.: Radiative
forcing of climate change, in: *Climate Change 1996, Contribution of Working Group I to
the 2nd Assessment Report of the Intergovernmental Panel on Climate Change*, edited
by: Houghton, J. T., Meira Filho, L. G., Callander, B. A., Harris, N., Kattenberg, A., and
25 Maskell, K., Cambridge University Press, Cambridge, UK and New York, NY, USA, 1996.
14091
- Spracklen, D. V.: Development and application of a Glomap Model of Aerosol Processes
(GLOMAP), Ph.D. thesis, University of Leeds, UK, 2005. 14097
- Spracklen, D. V., Pringle, K. J., Carslaw, K. S., Chipperfield, M. P., and Mann, G. W.: A global
30 off-line model of size-resolved aerosol microphysics: II. Identification of key uncertainties,
Atmos. Chem. Phys., 5, 3233–3250, doi:10.5194/acp-5-3233-2005, 2005. 14095
- Spracklen, D. V., Carslaw, K. S., Merikanto, J., Mann, G. W., Reddington, C. L., Picker-
ing, S., Ogren, J. A., Andrews, E., Baltensperger, U., Weingartner, E., Boy, M., Kulmala, M.,

**Global distribution of
CCN uncertainty**

L. A. Lee et al.

[Title Page](#)[Abstract](#)[Introduction](#)[Conclusions](#)[References](#)[Tables](#)[Figures](#)[◀](#)[▶](#)[◀](#)[▶](#)[Back](#)[Close](#)[Full Screen / Esc](#)[Printer-friendly Version](#)[Interactive Discussion](#)

Laakso, L., Lihavainen, H., Kivekäs, N., Komppula, M., Mihalopoulos, N., Kouvarakis, G., Jennings, S. G., O'Dowd, C., Birmili, W., Wiedensohler, A., Weller, R., Gras, J., Laj, P., Sellegri, K., Bonn, B., Krejci, R., Laaksonen, A., Hamed, A., Minikin, A., Harrison, R. M., Talbot, R., and Sun, J.: Explaining global surface aerosol number concentrations in terms of primary emissions and particle formation, *Atmos. Chem. Phys.*, 10, 4775–4793, doi:10.5194/acp-10-4775-2010, 2010. 14093

Stevens, R. G., Pierce, J. R., Brock, C. A., Reed, M. K., Crawford, J. H., Holloway, J. S., Ryerson, T. B., Huey, L. G., and Nowak, J. B.: Nucleation and growth of sulfate aerosol in coal-fired power plant plumes: sensitivity to background aerosol and meteorology, *Atmos. Chem. Phys.*, 12, 189–206, doi:10.5194/acp-12-189-2012, 2012. 14097

Stier, P., Feichter, J., Kinne, S., Kloster, S., Vignati, E., Wilson, J., Ganzeveld, L., Tegen, I., Werner, M., Balkanski, Y., Schulz, M., Boucher, O., Minikin, A., and Petzold, A.: The aerosol-climate model ECHAM5-HAM, *Atmos. Chem. Phys.*, 5, 1125–1156, doi:10.5194/acp-5-1125-2005, 2005. 14097

Textor, C., Schulz, M., Guibert, S., Kinne, S., Balkanski, Y., Bauer, S., Berntsen, T., Berglen, T., Boucher, O., Chin, M., Dentener, F., Diehl, T., Easter, R., Feichter, H., Fillmore, D., Ghan, S., Ginoux, P., Gong, S., Grini, A., Hendricks, J., Horowitz, L., Huang, P., Isaksen, I., Iversen, I., Kloster, S., Koch, D., Kirkevåg, A., Kristjansson, J. E., Krol, M., Lauer, A., Lamarque, J. F., Liu, X., Montanaro, V., Myhre, G., Penner, J., Pitari, G., Reddy, S., Seland, Ø., Stier, P., Takemura, T., and Tie, X.: Analysis and quantification of the diversities of aerosol life cycles within AeroCom, *Atmos. Chem. Phys.*, 6, 1777–1813, doi:10.5194/acp-6-1777-2006, 2006. 14091

Textor, C., Schulz, M., Guibert, S., Kinne, S., Balkanski, Y., Bauer, S., Berntsen, T., Berglen, T., Boucher, O., Chin, M., Dentener, F., Diehl, T., Feichter, J., Fillmore, D., Ginoux, P., Gong, S., Grini, A., Hendricks, J., Horowitz, L., Huang, P., Isaksen, I. S. A., Iversen, T., Kloster, S., Koch, D., Kirkevåg, A., Kristjansson, J. E., Krol, M., Lauer, A., Lamarque, J. F., Liu, X., Montanaro, V., Myhre, G., Penner, J. E., Pitari, G., Reddy, M. S., Seland, Ø., Stier, P., Takemura, T., and Tie, X.: The effect of harmonized emissions on aerosol properties in global models – an AeroCom experiment, *Atmos. Chem. Phys.*, 7, 4489–4501, doi:10.5194/acp-7-4489-2007, 2007. 14091

Global distribution of
CCN uncertainty

L. A. Lee et al.

Title Page

Abstract

Introduction

Conclusions

References

Tables

Figures

◀

▶

◀

▶

Back

Close

Full Screen / Esc

Printer-friendly Version

Interactive Discussion

**Table 1.** The model parameters and emissions, and their uncertainty ranges, used in this study.

Number	Short name	Parameter	Description	Uncertainty limits
X1	OX_DIAM	Oxidation activation diameter	Activation of aerosol to cloud droplets in stratiform clouds	[40,125] nm
X2	ACC_COEF	Mass accommodation coefficient	Probability that a molecule of H ₂ SO ₄ sticks to aerosol on collision	[0.02–1.00]
X3	NUC_THRESH	H ₂ SO ₄ nucleation threshold	Threshold concentration for new particles to be formed	[0.25–4.0] × baseline
X4	NUCRIT_SIZE	Nucleation critical cluster size	Smallest size above which a H ₂ SO ₄ cluster is stable	[50–100] molecules
X5	SO2_PART	Sulphate particulate emissions	% of sulphur emissions in each gridbox set to particulate	0–5 % of SO ₂
X6	SCAV_DIAM	Cloud nucleation scavenging diameter	Threshold for aerosol that can grow to rain droplets to be scavenged	[80–250] nm
X7	SO2_EMS	Sulphur emissions	Factor describing uncertainty in emissions inventory	70–130 % baseline
X8	SS_EMS	Sea spray emissions	Factor describing uncertainty in derived sea spray emissions	0.1–10 × baseline

Global distribution of
CCN uncertainty

L. A. Lee et al.

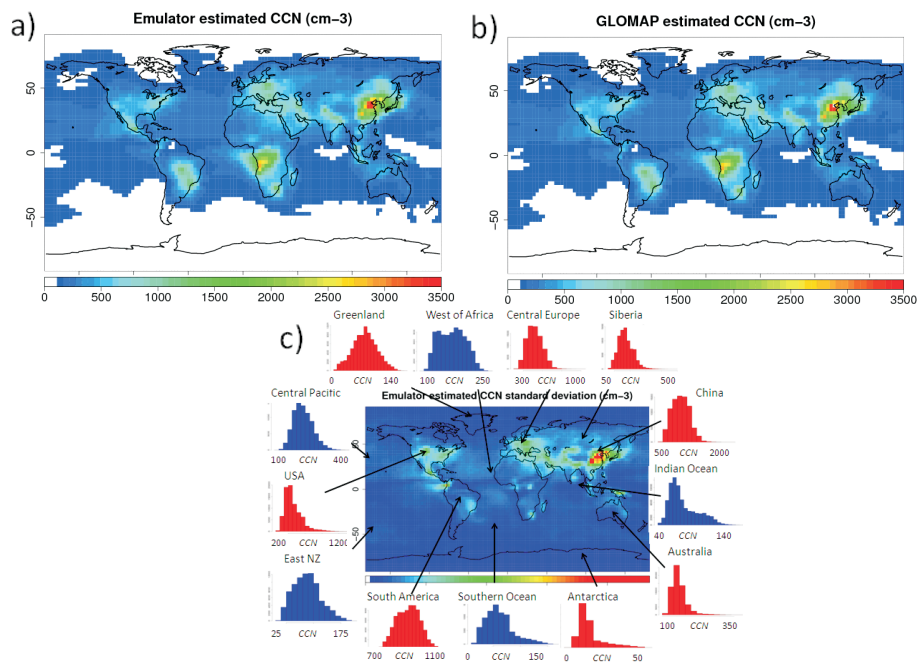


Fig. 1. Estimated July 2000 CCN from (a) the emulator and (b) the mean CCN from the 80 GLOMAP-mode runs. Panel (c) shows the uncertainty in the CCN (calculated as the standard deviation from the emulator) with posterior CCN distributions from the 80000 emulator simulations shown for 13 locations.

Title Page

Abstract

Introduction

Conclusions

References

Tables

Figures

◀

▶

◀

▶

Back

Close

Full Screen / Esc

Printer-friendly Version

Interactive Discussion



Global distribution of CCN uncertainty

L. A. Lee et al.

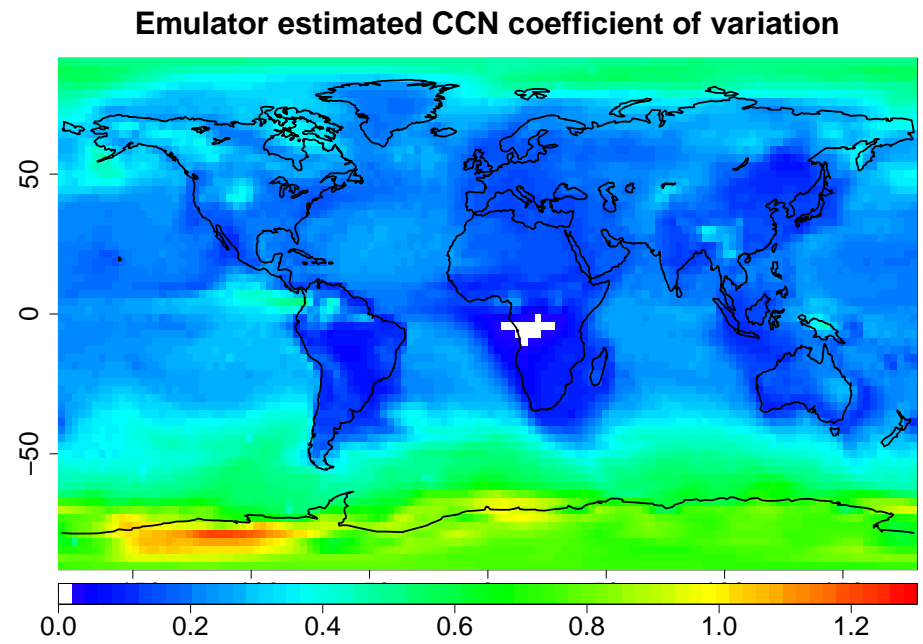


Fig. 2. The CCN coefficient of variation (σ/CCN) shows how well constrained the July 2000 CCN is in each gridbox with respect to the uncertainty in the 8 parameters in Table 1.

Title Page	
Abstract	Introduction
Conclusions	References
Tables	Figures
◀	▶
◀	▶
Back	Close
Full Screen / Esc	
Printer-friendly Version	
Interactive Discussion	



Global distribution of CCN uncertainty

L. A. Lee et al.

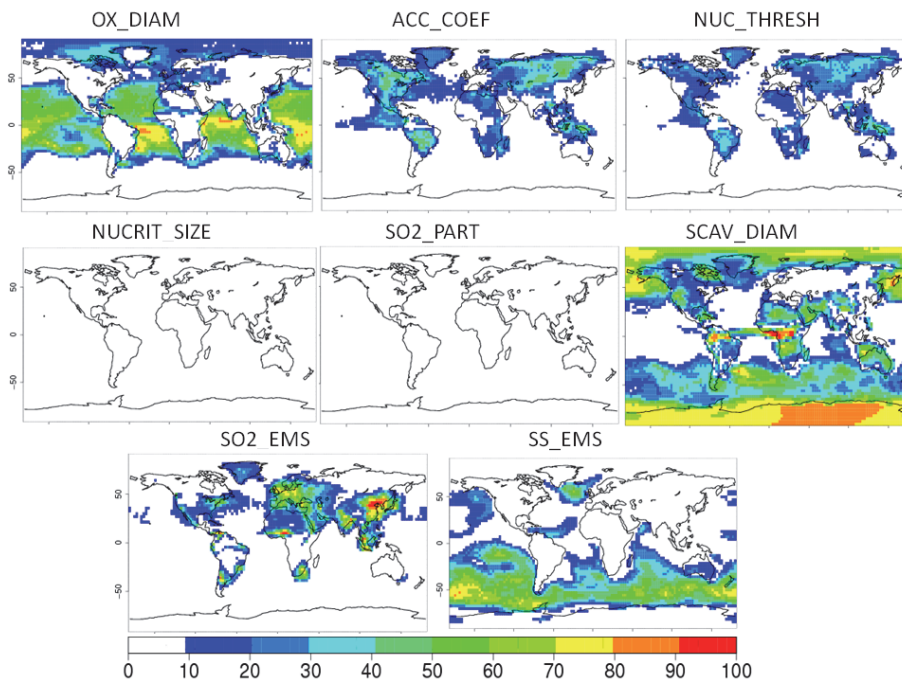


Fig. 3. Percentage of July 2000 CCN variance due to uncertainty in each of the 8 parameters in Table 1 – the main effect.

Title Page

Abstract Introduction

Conclusions References

Tables Figures

◀ ▶

◀ ▶

Back Close

Full Screen / Esc

Printer-friendly Version

Interactive Discussion



Global distribution of
CCN uncertainty

L. A. Lee et al.

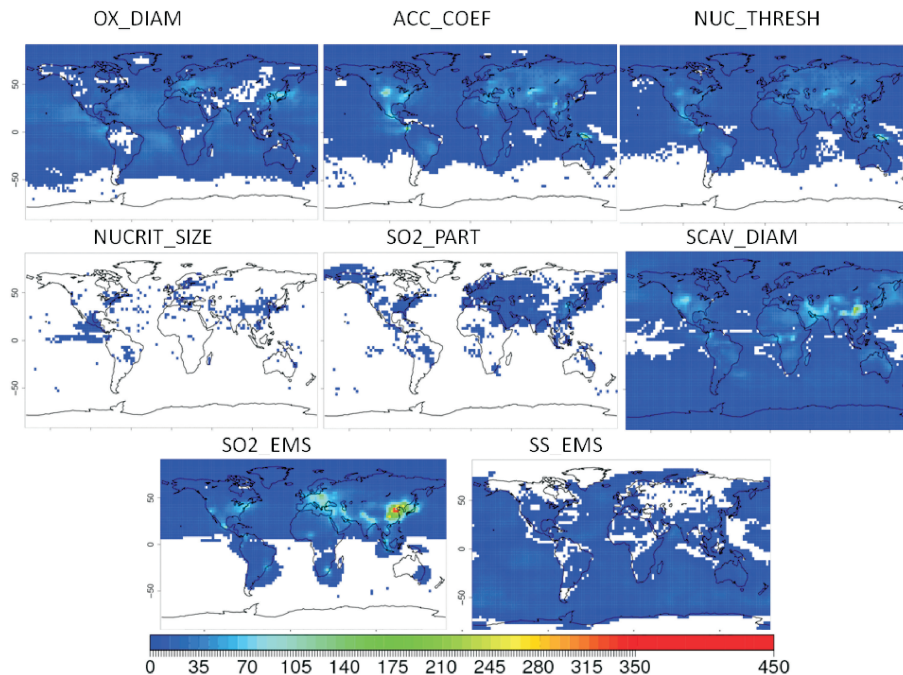


Fig. 4. The absolute July 2000 CCN standard deviation due to uncertainty in each of the 8 parameters in Table 1. The absolute standard deviation compared to the most sensitive parameters can help modellers choose which of the parameters is most important in the attempt to reduce uncertainty in global CCN modelling.

Title Page

Abstract

Introduction

Conclusions

References

Tables

Figures

◀

▶

◀

▶

Back

Close

Full Screen / Esc

Printer-friendly Version

Interactive Discussion



**Global distribution of
CCN uncertainty**

L. A. Lee et al.

Title Page

Abstract

Introduction

Conclusions

References

Tables

Figures

◀

▶

◀

▶

Back

Close

Full Screen / Esc

Printer-friendly Version

Interactive Discussion

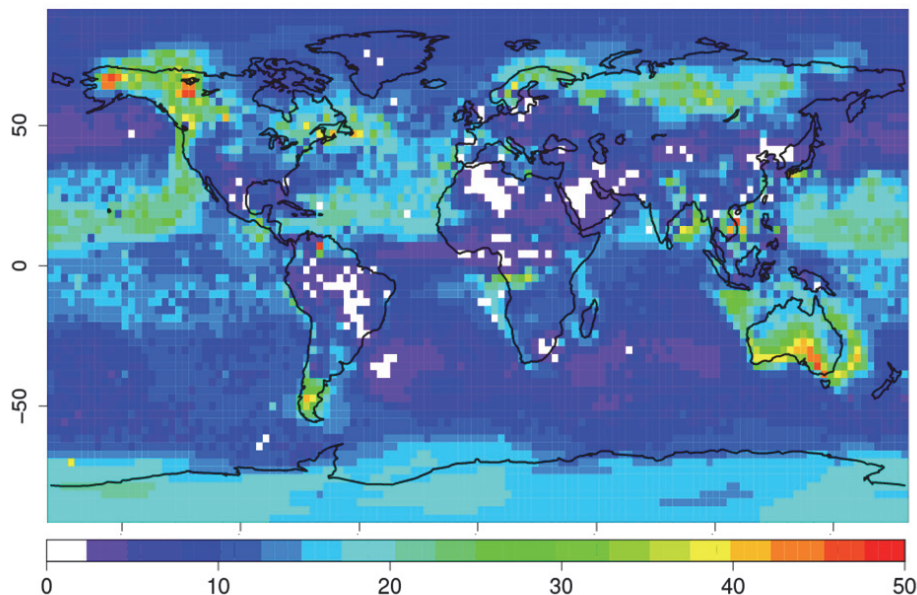
**% variance by all interaction effects**

Fig. 5. Percentage of July 2000 CCN variance not explained by the main effect of the 8 parameters in Table 1. This is the variance explained by the interaction of the 8 parameter uncertainties and cannot be captured using OAT tests.

Global distribution of
CCN uncertainty

L. A. Lee et al.

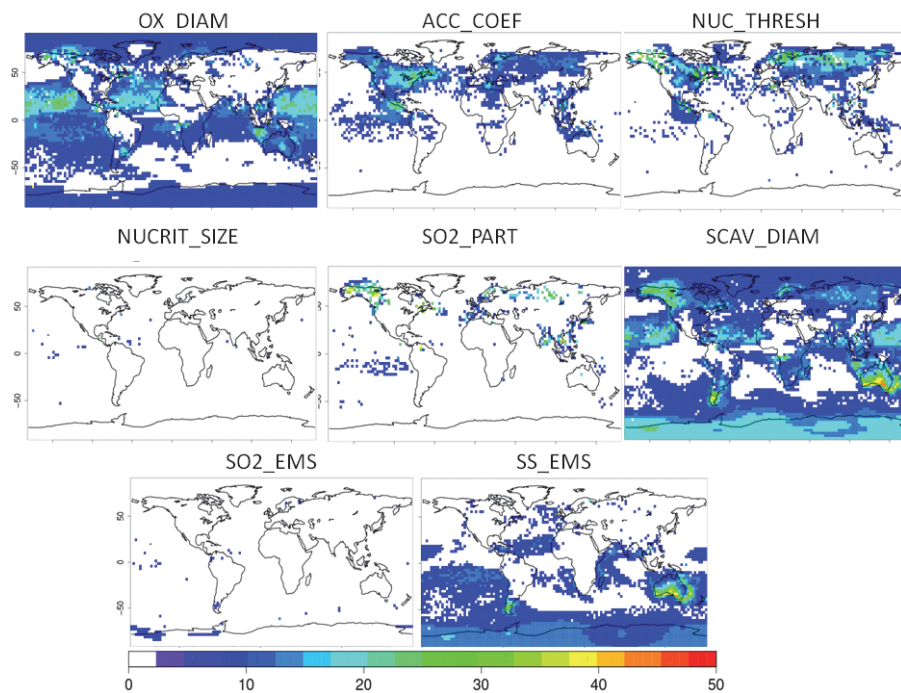


Fig. 6. The interaction effect of the individual parameters in Table 1 on July 2000 CCN uncertainty (calculated by the total effect minus the main effect).

[Title Page](#)[Abstract](#)[Introduction](#)[Conclusions](#)[References](#)[Tables](#)[Figures](#)[◀](#)[▶](#)[◀](#)[▶](#)[Back](#)[Close](#)[Full Screen / Esc](#)[Printer-friendly Version](#)[Interactive Discussion](#)

**Global distribution of
CCN uncertainty**

L. A. Lee et al.

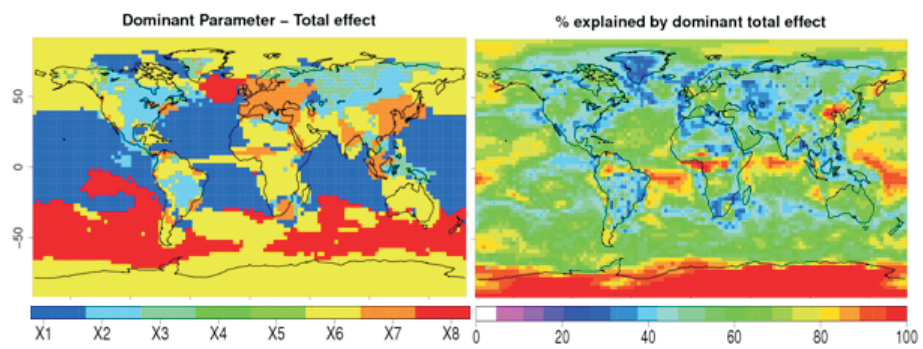


Fig. 7. The dominating total effect in each model gridbox and the percentage of July 2000 CCN variance explained by it.

Title Page

Abstract

Introduction

Conclusions

References

Tables

Figures

◀

▶

◀

▶

Back

Close

Full Screen / Esc

Printer-friendly Version

Interactive Discussion

